Carbohydrate Polymers 98 (2013) 1173–1178

Contents lists available at ScienceDirect

Carbohydrate Polymers

journal homepage: www.elsevier.com/locate/carbpol

Polyamidoamine dendrimer conjugated chitosan nanoparticles for the delivery of methotrexate

Zhen-Hua Leng[a,b,1], Qian-Fen Zhuang[b,1], Yan-Chao Li[b], Zeng He[c], Zhao Chen[b], Sai-Peng Huang[b], Hong-Ying Jia[b], Jian-Wei Zhou[a,**], Yang Liu[b,**], Li-Bo Du[b,*]

[a] School of Chemistry and Materials Science, Guizhou Normal University, Guiyang, Guizhou, China
[b] State Key Laboratory for Structural Chemistry of Unstable and Stable Species, Center for Molecular Science, Institute of Chemistry, Chinese Academy of Sciences, Beijing, China
[c] Institute of Blood Transfusion, Chinese Academy of Medical Sciences and Peking Union Medical College, Chengdu, Sichuan, China

ARTICLE INFO

Article history:
Received 14 February 2013
Received in revised form 9 July 2013
Accepted 9 July 2013
Available online 17 July 2013

Keywords:
Chitosan
Nanoparticles
PAMAM
Drug delivery
Methotrexate

ABSTRACT

Encapsulating anticancer drugs to synthetic polymer is a promising approach to improve the efficiency and reduce the side effects of anticancer drugs. In this study, novel chitosan derivatives with polyamidoamine moieties (CS-PAMAM) were synthesized and characterized by morphology, particle size, and zeta potential. Then the anticancer drug–methotrexate-encapsulated CS-PAMAM was prepared by hydrophobic–hydrophilic interactions. The drug release assay showed that the amount of the methotrexate release from CS-PAMAM was pH depended. Meanwhile, the cell viability assay illustrated that CS-PAMAM was suitable for the drug delivery because of its low cytotoxicity on cells. Moreover, our results showed that the CS-PAMAM could significantly improve the cytotoxicity of free methotrexate on A549 cells. These results demonstrate that CS-PAMAM may provide a suitable platform for the water-insoluble drug delivery.

1. Introduction

Methotrexate, as a proven chemotherapy drug, has been widely used in the treatment of malignancies including childhood acute lymphocytic leukemia, lung cancer, breast cancer, choriocarcinoma and related trophoblastic tumors (Murad et al., 1993; Natale et al., 1981). However, the clinical application of methotrexate is limited by its side-effects, such as toxicity to normal cells, acute and chronic hepatoxicity, and drug resistance (Calabresi & Parks, 1975). To solve these problems, advances have been made in encapsulating methotrexate into macromolecular carrier systems to reduce toxicity and overcome drug-resistance mechanisms.

Among these macromolecular carrier systems, poly(amidoamine) (PAMAM), as new class of artificial macromolecules with tree-like topological, nano-scale size, and surface functionality, have been widely used in biomedical fields such as drug delivery, gene transfection, and tissue engineering (Cheng, Zhao, Li, & Xu, 2011; Jia, Chen, Xu, Han, & Xu, 2009; Kumar, Muzzarelli, Muzzarelli, Sashiwa, & Domb, 2004; Menjoge, Kannan, & Tomalia, 2010; Svenson, 2009). However, the in vivo application of cationic PAMAM dendrimers is limited because of its high cytotoxicity on numerous cell lines and serious hemolytic activity on red blood, and also a rapid rate of blood clearance (Jones et al., 2012; Ziemba et al., 2012). To overcome these problems, much effort has been paid on improving the biocompatible and bioavaiablity of PAMAM through PEGylation, acetylation, glycosylation, etc. (Astruc, Boisselier, & Ornelas, 2010; Yu, Nie, Dohmen, Li, & Wagner, 2011). For instance, Soto-Castro, Cruz-Morales, Apan, and Guadarrama (2012) prepared a dendrimer using PAMAM as a central core and tris(hydroxymethyl)aminomethane as the functionalized units, which were used for the delivery of methotrexate, improving the anticancer activity of methotrexate. The functionalization of the PAMAM dendrimer on per-6-azido-β-cyclodextrin was achieved by Park et al. to reduce the toxic effect and improve the water-soluble and anticancer effect of the poorly water-soluble anticancer drug (methotrexate) (Deng et al., 2011).

On the other hand, in our previous study (Han et al., 2012), the chitosan nanoparticles (CSNPs) we prepared not only could improve the biocompatibility of antioxidants and enhance its antioxidant activity, but also illustrated a low in vitro cytotoxicity. We therefore speculated that the disadvantages of PAMAM which used as drug carriers may be resolved by conjugating PAMAM with

* Corresponding author. Tel.: +86 1062566306; fax: +86 1062559373.
** Corresponding authors.
E-mail addresses: jianweizhou_2000@yahoo.com (J.-W. Zhou), yliu@iccas.ac.cn (Y. Liu), dulibo@iccas.ac.cn (L.-B. Du).
[1] [1]These authors contributed equally to this work.

0144-8617/$ – see front matter © 2013 Elsevier Ltd. All rights reserved.
http://dx.doi.org/10.1016/j.carbpol.2013.07.021

the CSNPs. To test this hypothesis, the PAMAM conjugated CSNPs (CS-PAMAM) is synthesized and its cytotoxicity on different cell lines is evaluated.

Moreover, to evaluate whether the CS-PAMAM we prepared can be used for the delivery of anticancer drugs methotrexate, we then investigate the methotrexate delivery efficiency of CS-PAMAM and its drug effective on human lung adenocarcinoma epithelial cell line (A549 cells).

2. Materials and methods

2.1. Materials

Methotrexate, 1-ethyl-3-(3-dimethylaminopropyl) carbodiimide (EDC), 2-aminethanol, and ethylenediamine were purchased from Aldrich Chemical Co. and used as supplied. Chitosan (M_W = 80 kDa, degree of deacetylation = 85%) were purchased from Sinochem Co. Other chemicals were of reagent grade and used without further purification.

Mouse leukemic monocyte macrophage cell line (RAW 264.7), human lung adenocarcinoma epithelial cell line (A549 cells) were received from the American Type Culture Collection (Rockville, MD, USA) and cultured in Dulbecco's Modified Eagle Medium (Gibco, Grand Island, NY, USA) containing 10% fetal bovine serum (Hyclone, USA), 1 mM L-glutamine, and 100 U/mL streptomycin and penicillin. Cells were maintained at 37 °C in a 5% CO_2 humidified atmosphere.

Ultraviolet–vis (UV/vis) spectra were recorded in a conventional quartz cell (light path 10 mm) by using a Hitach UV-3310 spectrophotometer. ^{1}H NMR spectra were recorded at 400 MHz on a Bruker Advance II 400 spectrometer (Bruker, S.A., Wissembourg, Germany). Fourier transform infrared spectroscopy (FT-IR) was obtained by using a Bruker Tensor-27 Fourier-transform infrared spectrometer. The samples were prepared as tablets by using spectroscopic-grade KBr. ^{1}H NMR spectra were obtained with a Bruker AVANCE 400 NMR spectrometer in D_2O solution at room temperature. Elemental analyses were performed on a Flash EA 1112 instrument.

2.2. Synthesis of Boc-PAMAM (G4.0)

The Boc-protected PAMAM was synthesized according to the literature (Wang et al., 2004). Briefly, a solution of 2.0 g (12.48 mmol) N-Boc-ethylenediamine in 7.0 mL of methanol was added dropwise to a stirred solution of 4.33 g of methyl acrylate (49.92) in 8.0 mL of methanol at 0 °C. The resulting solution was then allowed to warm up to room temperature and stirred for 2 days. The solvent and the majority of the excess methyl acrylate were removed under reduced pressure using a rotary evaporator. The residue was further purified in vacuum oven for 2 days to give the final product as viscous yellowish oil (4.11 g, yield: 99%). Similar procedures were used for the preparation of Boc-protected PAMAM dendrons 4.0. ^{1}H NMR (D_2O, δ): 1.31 (9H, CCH_3), 2.39 (28H, $CH_2C{=}O$), 2.74 (62H, CH_2N), 3.12 (28H, NCH_2), 3.25 (32H, NCH_2), 3.41 (30H, $NHCH_2$).

2.3. Synthesis of PAMAM (G4.0)

Boc-protected PAMAM (4.0 g, 12.03 mmol) was dissolved in 20 mL of methanol and was then added dropwise to a cold (0 °C) 30 mL methanol solution containing HCl (0.1 M) over a period of 1 h. The reaction mixture was allowed to warm up to room temperature and stirred for 6 h. Afterwards, the solvent was removed under reduced pressure using a rotary evaporator. The residue was dried in a vacuum oven for 1 day to give the amino-terminated product as a honey-like oil (4.58 g, yield: 98%). ^{1}H NMR (D_2O, δ): 2.36 (28H, $CH_2C{=}O$), 2.72 (62H, CH_2N), 3.11 (28H, NCH_2), 3.24 (32H, NCH_2), 3.39 (30H, $NHCH_2$).

2.4. The synthesis of CS-PAMAM and methotrexate–CS-PAMAM

PAMAM was conjugated with CSNPs according to the reported method with minor modification (Chiou & Wu, 2006). Briefly, in a round bottom flask, 21 μM EDC was weighted. 20 mL aqueous solution of chitosan (Han et al., 2012) was added and the mixture was stirred at 20 °C for 30 min. The excess EDC was removed by dialysis. Then 21 μM PAMAM were added under stirring, and the reaction was kept at 20 °C for 2 h. After removing the excess PAMAM and by products with dialysis, the CS-PAMAM were obtained and characterized by FT-IR, elemental analysis and ^{1}H NMR.

For the preparation of methotrexate–CS-PAMAM, lyophilized powder of CS-PAMAM (30 mg) was dissolved in PBS (2.5 mL, pH 7.4). Methotrexate (13–15 mg) was then added into CS-PAMAM and stirred at 1000–2000 rpm/min for 2 h under nitrogen. The obtained methotrexate–CS-PAMAM was subsequently collected by ultra-centrifugation (Himac CP80MX, Hitachi, Japan) in eppendorf tubes at 58,000 rpm and 4 °C for 30 min. The methotrexate–CS-PAMAM were washed twice with PBS and dried in a freeze dryer (FD-1C-50, Boyikang Co., Ltd., China) for further usage. The methotrexate–CS-PAMAM dispersed in PBS was detected at 303 nm to determine the concentration of methotrexate encapsulated.

2.5. The MTT assay

Typically, 6×10^4 A549 cells were seeded in 96-well plates and cultured in Minimum Essential Medium Eagle (MEM, Hyclone, Logan, UT) with Earle's balance salt and L-glutamine, supplemented with 10% fetal bovine serum (FBS, Invitrogen, Grand Island, NY) and 1% penicillin/streptomycin (PS, Invitrogen, Grand Island, NY) at 37 °C under 5% CO_2. After 24 h, the cells were washed with 100 μL of serum-free MEM (1% PS) twice and incubated with 100 μL of different concentrations of methotrexate, methotrexate–CS-PAMAM suspensions in serum-free MEM (1% PS). After 72 h exposure, the cells were washed twice with 100 μL of serum-free MEM and incubated with 100 μL of 0.5 mg/mL methylthiazolyldiphenyl-tetrazolium bromide (MTT, Invitrogen, Eugene, OR) containing media for 2 h at 37 °C under 5% CO_2. Finally, the MTT containing media was removed and the insoluble purple formazan crystals produced by live cells were dissolved in 100 μL of dimethyl sulfoxide (DMSO, Sigma–Aldrich, Milwaukee, WI). The plate was placed on a rocking shaker for at least 20 min and then 80 μL of the purple DMSO solution in each well was transferred to a new 96-well plate. Optical density of the produced stain was monitored at 570 nm, with 655 nm as a reference, using an iMark microplate reader (Bio-Rad, Hercules, CA).

2.6. In vitro release studies

Prepared methotrexate–CS-PAMAM were dispersed in PBS (5 mL, pH 7.4 or pH 5.5) and subjected to dialysis membrane (molecular weight cutoff 1000) in vials containing 30 mL PBS, and further they were maintained at 37 °C in a shaking incubator at a shaking speed of 100 ± 1 rpm. At predetermined time intervals, 1 mL medium from the vial were collected and replaced with fresh PBS. Collected samples were measured at 288 nm by UV–vis spectrophotometer (UV 3310, Hitachi). All measurements were performed in triplicate.

2.7. Platelet aggregation and activation tests

2.7.1. Research donor blood

If not specified otherwise, healthy volunteer blood specimens were drawn under NCI-Frederick Protocol OH99-C-N046. Blood was collected in BD vacutainer tubes containing sodium citrate as anticoagulant. To avoid individual variability, plasma from at least three donors was pooled.

2.7.2. Cell counter based screening method

To study nanoparticles effects on platelet aggregation, whole blood was centrifuged 8 min at 200 × *g* in order to obtain platelet rich plasma (PRP). PRP was treated with nanoparticles (PAMAM, CS, and CS-PAMAM), PBS (negative control) or collagen (positive control) for 15 min at 37 °C. After that single platelet count was conducted using a Z2 counter and size analyzer (Beckman Coulter). The difference in single platelet count between negative control and test samples was used to calculate percent platelet aggregation. Additional control included incubation of platelet poor plasma and PBS with particles and analyzing these samples on the instrument. These controls were used to monitor potential particle aggregation in the presence of plasma proteins to avoid false-negative results.

2.7.3. Flow cytometry

Analysis of platelet surface activation markers and platelet membrane microparticles (MPs) by flow cytometry were as described previously (Semberova et al., 2009). Platelet rich plasma was prepared as described above and then diluted to 250×10^3 platelets/μL with platelet poor plasma for microparticle experiments and to 30×10^3 platelets/μL with Tyrode's–HEPES buffer (THB: 130 mM NaCl, 2.6 mM KCl, 0.42 mM NaH_2PO_4, 5.5 mM glucose, 10 mM HEPES, 0.3% bovine serum albumin) for assessing platelet surface activation markers. Platelets were equilibrated for 30 min after dilution. Then they were incubated with tested nanomaterials (100 μg/mL) or a positive/negative control (20 μM TRAP-6 and platelets only, respectively) for 15 min on a rocking platform at 37 °C. Platelet surface markers and MP assays were run in parallel, using the same blood specimen. For analysis of platelet surface markers, platelet samples were spun briefly for 1 min, at 150 g at room temperature to avoid the presence of large nanomaterial aggregates. Fifty microliters of supernatant was stained with saturating concentration of monoclonal antibodies against CD62P (PE labeled). Matching isotype controls and non-labeled samples were used as controls. After 15 min incubation in the dark, at room temperature, samples were diluted 10-fold with THB and immediately acquired using a FACS Calibur flow cytometer (Becton Dickinson, San Diego, CA, USA) equipped with CELLQuest software, with forward scatter (FSC) and side scatter (SSC) in logarithmic mode and subsequently analyzed using FlowJo (Tree Star, Inc., Ashland, OR). Representative histograms and FSC/SSC plots of 3 independent experiments are presented.

Microparticle samples, after incubation with nanomaterials (PAMAM, CS, CS-PAMAM), were spun for 10 min at 10 °C at 10,000 × *g* to obtain platelet free plasma (PFP) for the MP assay. Samples were then processed and analyzed as described previously (Gelderman & Simak, 2008; Simak, Gelderman, Yu, Wright, & Baird, 2006). Aliquots of 50 μL of PFP were incubated for 20 min at room temperature in the dark with saturating concentrations of PE conjugated antibodies. In parallel, non-labeled samples and samples labeled with relevant isotype controls were analyzed. After incubation and washing with 1 mL of HBSS/Ca^{2+}/BSA, samples were resuspended in 500 μL of HBSS/Ca^{2+}/BSA (Hanks balanced salt solution, Gibco, Grand Island, NY, was supplemented with $CaCl_2$ to 2.5 mM Ca^{2+} and with 0.3% BSA) and analyzed by flow cytometry. Data were acquired using the flow cytometer and software as described above. MPs were analyzed using both forward scatter (FSC) and side scatter (SSC) in logarithmic mode. The flow rate was evaluated using TruCount beads from Becton Dickinson (San Diego, CA) analyzed as separate samples in parallel. MPs were defined as particles ≤1 μm based on size comparison on forward scatter with the size standard polystyrene beads of 1 μm in diameter. Counts of CD62P and in the platelet supernatant were evaluated using double fluorescence plots acquired for 60 s at the standard flow rate. Relative increase in MP count in platelet supernatant after different treatments is presented as mean ± SEM of three independent experiments. Representative double fluorescence plots of MPs are shown.

2.8. Cellular uptake of FITC–CS-PAMAM

For investigating the kinetics of cellular uptake, CS-PAMAM was labeled with FITC by using a protocol previously described. RAW 264.7 cells were plated on a 35 mm confocal dish at a density of 5.0×10^5 cells/dish at 37 °C for 12 h. Then, the growth medium was replaced with 2 mL of the pre-prepared FITC–CS-PAMAM solution in complete culture medium. After 1 h, 2 h and 4 h incubation, the cells were washed with PBS for three times. Subsequently, the cells were washed again with PBS for three times and imaged at 100× magnification using laser confocal microscopy (FV1000-IX81, Olympus).

3. Results and discussion

3.1. Synthesis and characterization of CS-PAMAM

CS-PAMAM was synthesized by reacting the primary amino groups of PAMAM dendrimer with CSNPs. Fig. 1 shows the FT-IR spectra of the PAMAM, CSNPs, and CS-PAMAM. For PAMAM, the characteristic absorption bands which appeared in the wavenumber region of 1734 cm^{-1} can be assigned to the ester carbonyl group of the PAMAM. After it conjugated with CSNPs, a new peak which belongs to C—O—C at 1280 cm^{-1} appeared. This result indicates that the PAMAM has been conjugated on the chitosan. Moreover, ^1H NMR was used to further confirm the surface capping of the terminal amines of the CSNPs with PAMAM. The ^1H NMR of the CSNPs shows six broad peaks, which correspond to the protons of the methylene group next to hydroxyl group at 3.01 ppm, the internal CH/CH_2 groups in the chitosan ring at 3.61–4.0 ppm. The ^1H NMR spectrum of PAMAM clearly shows five peaks. The peak at 2.47 ppm is the resonance of protons of the CH_2 at position —$NCH_2C\boldsymbol{H_2}CO$—. The peak at 3.54 ppm belongs to the CH_2 at position —$CONHC\boldsymbol{H_2}CH_2N$—. Compared with the spectrum of the PAMAM and CSNPs, the NMR spectrum of the CS-PAMAM shows that the PAMAM has been conjugated with CSNPs.

Moreover, the macromolecular structure of the polymers has also been studied by the C/H/N ratio. The C/H/N ratio of CSNPs, PAMAM, and CS-PAMAM were calculated and listed in Table 1. The results showed that the percentage of PAMAM in the nanoparticles prepared with the CS-PAMAM concentration of 10.0 mg/mL was about 4.6% (w/w).

DLS, TEM and zeta potential measurements were performed to further understand the size, the morphologies and the surface charge properties of the resulting product CS-PAMAM. According to the DLS results (Fig. 1c), the hydrodynamic size of methotrexate–CS-PAMAM was 86.2 ± 21.2 nm, increasing from 76.1 ± 18.2 nm of empty CS-PAMAM, which was likely to be caused by encapsulating methotrexate into CS-PAMAM. Although the particles of CS-PAMAM gave relatively high scattering intensity in solution, most of carriers still stay at the small diameter because the scattering intensity was proportional to the 2.5 time of the particle size (Han et al., 2012). Moreover, TEM images further

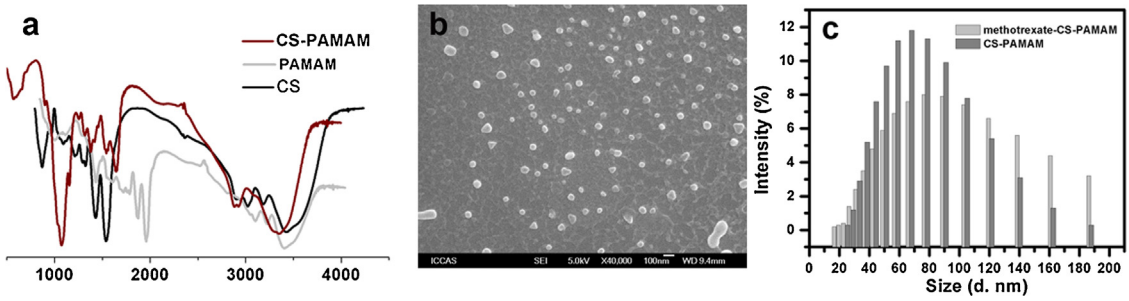

Fig. 1. (a) The FT-IR spectra of chitosan, PAMAM and CS-PAMAM. (b) Representative TEM image of CS-PAMAM negatively stained with uranyl acetate. (c) DLS intensity plots of empty CS and CS-PAMAM.

Table 1
The elements analysis of CS-PAMAM, PAMAM and Methotrexate-CS-PAMAM.

Compounds	Element percent%			
	C	H	O	N
CS-PAMAM	40.75 ± 0.18	8.13 ± 0.07	36.97 ± 0.08	14.15 ± 0.12
PAMAM	41.46 ± 0.13	6.91 ± 0.04	43.96 ± 0.11	7.67 ± 0.05
Methotrexate–CS-PAMAM	44.31 ± 0.09	8.15 ± 0.14	31.87 ± 0.10	15.67 ± 0.02

proved that the particles in solution were loosely associated rather than the larger diameter aggregates (Fig. 2b), and the size of CS-PAMAM from TEM was consistent well with the particle size of 30–50 nm measured by DLS measurements. The zeta potential measurement showed the charge values of PAMAM and CS-PAMAM were 21 ± 2.1 mV and 22 ± 1.1 mV, indicating that the encapsulation of methotrexate into PAMAM did not influence the surface charge of PAMAM. As we known, the presence of positive-charged CS-PAMAM can enhance their binding to negatively charged cell surfaces by electrostatic interactions, which may increase the chance of CS-PAMAM entered into cells.

3.2. Drug release in vitro

The dynamic of methotrexate release from methotrexate–CS-PAMAM was investigated under different pHs (pH 5.5, pH 7.4) conditions at 37 °C. The results showed that at pH 7.4, the release rate of methotrexate from methotrexate–CS-PAMAM is extremely low, only 35% of the methotrexate released out of the dialysis bag after 24 h. The reason may be attributed to the strong hydrophobic hydrophilic interactions between methotrexate and CS-PAMAM, thereby resulting in the slower release of methotrexate from methotrexate CS-PAMAM (Kannaiyan & Imae, 2009). In addition, many previous studies have been illustrated that the release of drugs from dendrimers can be tailored by changing the pH condition of the release system (Richardson, Ferruti, & Duncan, 1999; Wan et al., 2004). In this study, as expected, at pH 5.5, most of methotrexate (38%) from methotrexate–CS-PAMAM was released within 2 h and reach a plateau after 5 h (58%). The reason for the higher release rate of methotrexate in an acid environment can be attributed to the quaternization of tertiary amine groups in the interior pockets of CS-PAMAM. The quaternization process decreases the hydrophobicity of CS-PAMAM and then increases the dendrimer volume, thereby resulting in the release of the encapsulated anticancer drugs (Hu, Cheng, Ma, Wu, & Xu, 2009). It has been demonstrated that dendrimer and dendrimer/drug complexes are generally transported into endosomes after cellular uptake. The pH values of endosomes can drop below pH 5.0

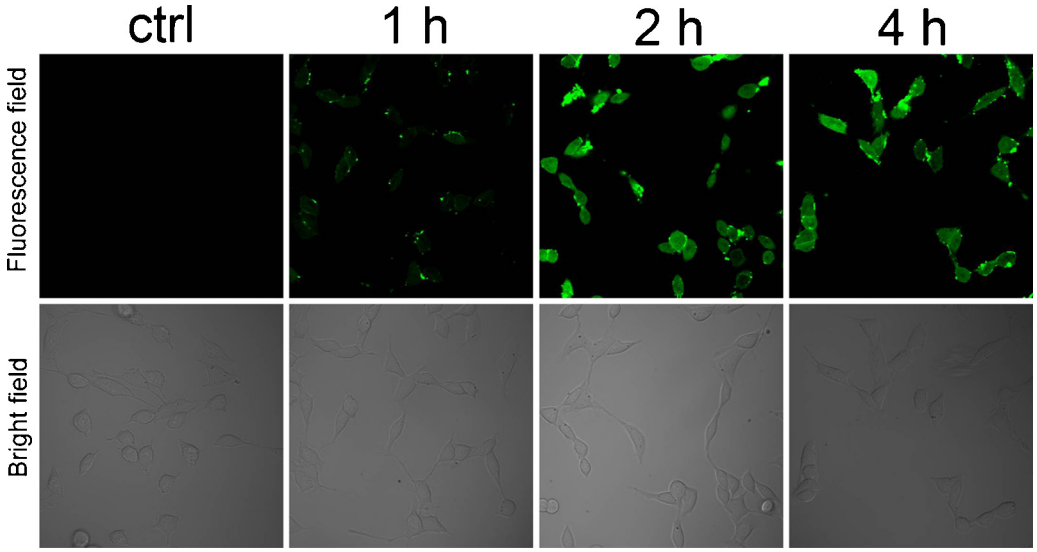

Fig. 2. Intracellular trafficking of CS-PAMAM in RAW 264.7 cells were incubated with FITC–CS-PAMAM for 1 h, 2 h and 4 h. After 1 h of incubation, only small amount of CS-PAMAM were phagocytized by cells while many CS-PAMAM entered into cells after 2 h incubation.

(Saovapakhiran, D'Emanuele, Attwood, & Penny, 2009), which can stimulate the release of encapsulated anticancer drugs from dendrimers or chitosan. Thus, it can be inferred that CS-PAMAM, which was characteristic of responding to mildly acidic condition, was useful vehicles for the drug delivery in biological environment, i.e., late endosomes and lysosomes.

3.3. Intracellular tracking of CS-PAMAM

Macrophages (i.e., RAW 264.7 cells) are our first line of defense and play the pivotal role in our immune response to any attack by any intruder (Ezekowitz et al., 1991). Therefore, to track CS-PAMAM following their uptake, RAW 264.7 cells, used as a cell model, were treated with FITC-labeled CS-PAMAM (FITC–CS-PAMAM). The results showed that the cellular uptake of FITC–CS-PAMAM by RAW 264.7 cells was time-dependent. Specifically, as shown in Fig. 2, after 2 h incubation, accumulation of FITC–CS-PAMAM within the cytoplasm were observed in most of incubated RAW 264.7 cells, which suggested that CS-PAMAM could cross cell membranes by cellular endocytosis and localize in intracellular compartments. Our previous study has been demonstrated that the CSNPs can be translocated in the lysosome via lysosome pathway after cellular uptake (Han et al., 2012). In addition, some previous studies also showed that the PAMAM dendrimer were localized in the lysosome after cellular uptake (Saovapakhiran et al., 2009). We therefore speculated that the internalized CS-PAMAM would be translocated via lysosome pathway after entering cells. The environment of late endosome or lysosome is acidic (below pH 5.0), where the internalized methotrexate–CS-PAMAM disassembled, resulting in a burst release of methotrexate from CS-PAMAPM into cytoplasm.

3.4. In vitro cytotoxicity of the CS-PAMAM

Before nanoparticles can be considered for the use in vivo, the cytotoxicity of the nanoparticles should be seriously considered firstly (Brigger, Dubernet, & Couvreur, 2002). In this paper, to evaluate the cytotoxicities of CS-PAMAM, the cell viability of RAW264.7 cells treated by CS-PAMAM was investigated using an MTT assay. Untreated cells as well as cells treated with different concentrations of CS-PAMAM were subjected to the MTT assay for cell viability determination. After 72 h of post-treatment, CS-PAMAM did not show any appreciable cytotoxicity (the percent of cell viability was over 96.03 ± 0.41%), even at a concentration of 2 mg/mL, which are a much higher concentration that encountered in many other studies, indicating that CS-PAMAM are low toxicity and good biocompatibility. However, the cytotoxicity of PAMAM on RAW264.7 cells arises due to the cationic surface of the dendrimer (the percent of cell viability was only 67.22 ± 1.21% at the concentration of 2 mg/mL). Certainly, some previous studies have also found the similar results (Albertazzi et al., 2012; Janaszewska et al., 2012). These results suggest that CS-PAMAM have quiet low cytotoxicity and might be one of the most versatile polymers for drug delivery with minimal toxicity.

After demonstrating the low cytotoxicity of CS-PAMAM on RAW264.7, we further evaluated the anticancer drug delivery efficiency of CS-PAMAM using methotrexate as the model drug. As shown in Fig. 3, 3.2 mg/mL methotrexate induced 48% A549 cell death. Comparatively, methotrexate–CS-PAMAM exerts a higher cytotoxic effect than methotrexate on A549 cells at concentrations above 0.2 mg/mL (the concentration of methotrexate). Apparently, the IC_{50} value of 0.8 mg/mL for methotrexate–CS-PAMAM is obviously lower than that for the methotrexate (~4.54 mg/mL) (Santos et al., 2007). On the other hand, it is well known that the side effects of anticancer drugs can be significantly reduced when the drugs are given below its maximum tolerance dose (Lee et al., 2006). In this study, as shown in Fig. 3b, it is worth noticing that

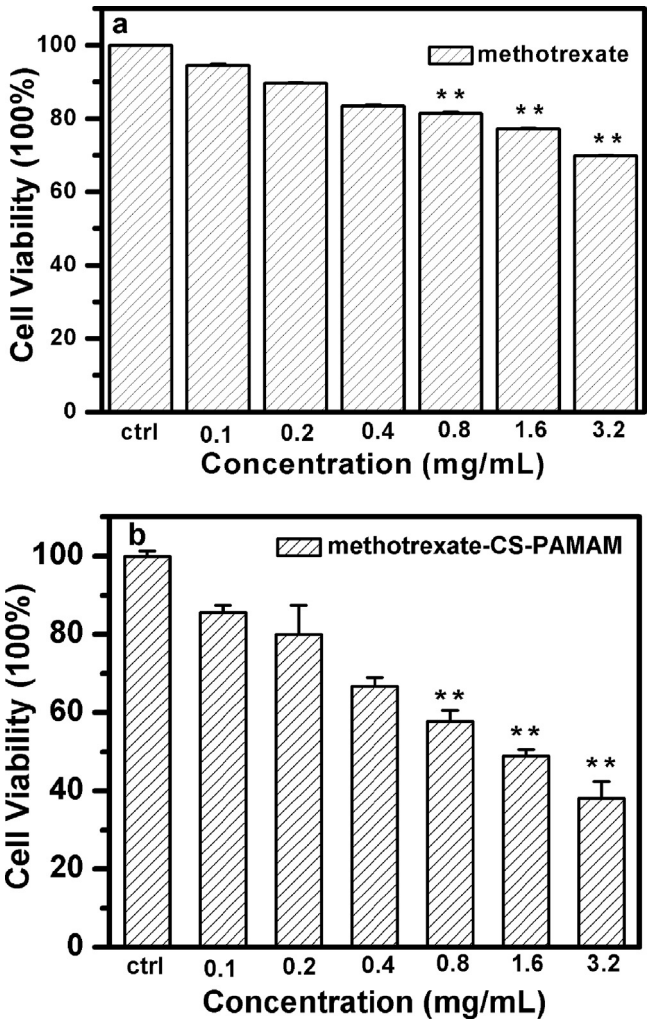

Fig. 3. Relative cell viability of A549 cells treated with methotrexate (a) and methotrexate–CS-PAMAM (b). The data shown are mean ± S.D. from at least six independent experiments, each performed in triplicate. $^{**}P < 0.01$ versus control.

the methotrexate–CS-PAMAM showed a much lower cytotoxicity (less than 30%) when the concentration of MTX reached 0.4 mg/mL. The results indicated that the PAMAM-chitosan may effectively improve the maximum tolerance dose of methotrexate in clinical trials and provide an alternative way for the delivery of water insoluble anticancer drugs.

3.5. Platelet aggregation in vitro

As we known, previous studies demonstrated that the PAMAM could induce platelet aggregation and cause toxicity, thereby restricting their in vivo application (Dobrovolskaia et al., 2012; Roberts, Bhalgat, & Zera, 1996). In this study, further considering that the chitosan have capacity to stabilizes platelet growth factors (Busilacchi et al., 2013), to investigate whether the PAMAM induced platelet aggregation could be relieved by conjugating PAMAM on the CSNPs, CS-PAMAM were added to purified platelets for 30 min, and then the platelets aggregation were measured. We did not observe apparent platelet aggregation in platelet rich plasma treated with CSNPs (5.93 ± 1.73%) and CS-PAMAM dendrimers (6.31 ± 0.62%) at a concentration of 2 mg/mL; however, their cationic counterparts PAMAM resulted in platelet aggregation in the same concentration (23.52 ± 3.25%). This data are in agreement with an earlier PAMAM dendrimer study which showed that cationic PAMAM dendrimers were cytotoxic and caused lysis of red

blood cells (Malik et al., 2000). Moreover, P-selectin, which located on the inner wall of α-granules, is very important in the recruitment and aggregation of platelets. Generally, the release of P-selectin can promotes platelet aggregation through platelet–fibrin and platelet–platelet binding. As a membrane of the selectin family, CD62P (a platelet granule membrane protein) could be used as the marker for the platelet aggregation. The result shows that platelets treated with CS-PAMAM exhibited very little CD62P expression after 30-min incubation ($6.37 \pm 0.33\%$), while platelets treated with PAMAM elicited significantly higher levels of CD62P expression ($45.79 \pm 0.35\%$). All these results indicated that platelet aggregation induced by PAMAM can be relieved by conjugating PAMAM on the chitosan. Perhaps more importantly, the results demonstrated that CS-PAMAM may provide an alternative way for the resolve of the platelet aggregation induced by PAMAM dendrimer.

4. Conclusion

The CS-PAMAM and methotrexate–CS-PAMAM have been synthesized. The methotrexate–CS-PAMAM is pH-responsive drug release systems, which enabled pH-controlled activation of the methotrexate in buffering modeling environment in lysosomes of tumor cells. The in vitro studies performed on RAW 264.7 showed that the CS-PAMAM has low cytotoxicity. Further anticancer efficiency studies demonstrated that the methotrexate–CS-PAMAM can increase the anticancer activity of methotrexate by increasing the drug delivery efficiency into cells. We believe this strategy can make unique applications of CS-PAMAM in particular when targeting a non-cytosolic therapeutic system localized in a subcellular compartment such as nucleus into which nanoscale particles are unable to passively cross (Kukowska-Latallo et al., 2012).

Disclosures

The authors declare no conflicts of interest. The authors alone are responsible for the content and writing of the paper. None of the authors has a financial conflict of interest related to this research.

Acknowledgements

This project was supported by the National Natural Science Foundation of China (No. 91227122 and 21063004).

References

Albertazzi, L., Gherardini, L., Brondi, M., Sato, S. S., Bifone, A., Pizzorusso, T., et al. (2012). In vivo distribution and toxicity of PAMAM dendrimers in the central nervous system depend on their surface chemistry. *Molecular Pharmaceutics*, *10*, 249–260.

Astruc, D., Boisselier, E., & Ornelas, C. (2010). Dendrimers designed for functions: From physical, photophysical, and supramolecular properties to applications in sensing, catalysis, molecular electronics, photonics and nanomedicine. *Chemical Reviews*, *110*, 1857–1959.

Brigger, I., Dubernet, C., & Couvreur, P. (2002). Nanoparticles in cancer therapy and diagnosis. *Advanced Drug Delivery Reviews*, *54*, 631–651.

Busilacchi, A., Gigante, A., Mattioli-Belmonte, M., Manzotti, S., & Muzzarelli, R. A. A. (2013). Chitosan stabilizes platelet growth factors and modulates stem cell differentiation toward tissue regeneration. *Carbohydrate Polymers*, *98*, 665–676.

Calabresi, P., & Parks, R. E. (1975). *The pharmacological basis of therapeutics*. Macmillan: New York.

Cheng, Y. Y., Zhao, L. L., Li, Y. Y., & Xu, T. W. (2011). Design of biocompatible dendrimers for cancer diagnosis and therapy: Current status and future perspectives. *Chemical Society Reviews*, *40*, 2673–2703.

Chiou, S.-H., & Wu, W.-T. (2006). Immobilization of *Candida rugosa* lipase on chitosan with activation of the hydroxyl groups. *Biomaterials*, *25*, 197–204.

Deng, J., Li, N., Mai, K., Yang, C., Yan, L., & Zhang, L. (2011). Star-shaped polymers consisting of a b-cyclodextrin core and poly(amidoamine) dendron arms: Binding and release studies with methotrexate and siRNA. *Journal of Materials Chemistry*, *21*, 5273–5281.

Dobrovolskaia, M. A., Patri, A. K., Simak, J., Hall, J. B., Semberova, J., De Paoli Lacerda, S. H., et al. (2012). Nanoparticle size and surface charge determine effects of PAMAM dendrimers on human platelets in vitro. *Molecular Pharmaceutics*, *9*, 382–393.

Ezekowitz, R. A. B., Williams, D. J., Koziel, H., Armstrong, M. Y. K., Warner, A., Richards, F. F., et al. (1991). Uptake of *Pneumocystis carinii* mediated by the macrophage mannose receptor. *Nature*, *351*, 155–158.

Gelderman, M. P., & Simak, J. (2008). Flow cytometric analysis of cell membrane microparticles. *Methods in Molecular Biology*, *484*, 79–93.

Han, L., Du, L. B., Kumar, A., Jia, H. Y., Liang, X. J., Tian, Q., et al. (2012). Inhibitory effects of trolox-encapsulated chitosan nanoparticles on tert-butylhydroperoxide induced RAW264.7 apoptosis. *Biomaterials*, *33*, 8517–8528.

Hu, J. J., Cheng, Y. Y., Ma, Y. R., Wu, Q. L., & Xu, T. W. (2009). Host–guest chemistry and physico-chemical properties of dendrimer–mycophenolic acid complexes. *Journal of Physical Chemistry B*, *113*, 64–74.

Janaszewska, A., Maczyńska, K., Matuszko, G., Appelhans, D., Voit, B., Klajnert, B., et al. (2012). Cytotoxicity of PAMAM, PPI and maltose modified PPI dendrimers in Chinese hamster ovary (CHO) and human ovarian carcinoma (SKOV3) cells. *New Journal of Chemistry*, *36*, 428–437.

Jia, X., Chen, X., Xu, Y., Han, X., & Xu, Z. (2009). Tracing transport of chitosan nanoparticles and molecules in Caco-2 cells by fluorescent labeling. *Carbohydrate Polymers*, *78*, 323–329.

Jones, C. F., Campbell, R. A., Franks, Z., Gibson, C. C., Thiagarajan, G., Vieira-de-Abreu, A., et al. (2012). Cationic PAMAM dendrimers disrupt key platelet functions. *Molecular Pharmaceutics*, *9*, 1599–1611.

Kannaiyan, D., & Imae, T. (2009). PH-dependent encapsulation of pyrene in PPI-core: PAMAM-shell dendrimers. *Langmuir*, *25*, 5282–5285.

Kumar, M. N. V. R., Muzzarelli, R. A. A., Muzzarelli, C., Sashiwa, H., & Domb, A. J. (2004). Chitosan chemistry and pharmaceutical perspectives. *Chemical Review*, *104*, 6017–6084.

Kukowska-Latallo, J. F., Candido, K. A., Cao, Z., Nigavekar, S. S., Majoros, I. J., Thomas, T. P., et al. (2012). Nanoparticle targeting of anticancer drug improves therapeutic response in animal model of human epithelial cancer. *Cancer Research*, *65*, 5317–5324.

Lee, C. C., Gillies, E. R., Guillaudeu, S. J., Fréchet, J. M. J., Dy, E. E., & Szoka, F. C. (2006). A single dose of doxorubicin-functionalized bow-tie dendrimer cures mice bearing C-26 colon carcinomas. *Proceedings of the National Academy of Sciences of the United States of America*, *103*, 16649–16654.

Malik, N., Wiwattanapatapee, R., Klopsch, R., Lorenz, K., Frey, H., Weener, J. W., et al. (2000). Dendrimers: Relationship between structure and biocompatibility in vitro, and preliminary studies on the biodistribution of 125I-labelled polyamidoamine dendrimers in vivo. *Journal of Controlled Release*, *65*, 133–148.

Menjoge, A. R., Kannan, R. M., & Tomalia, D. A. (2010). Dendrimer-based drug and imaging conjugates: Design considerations for nanomedical applications. *Drug Discovery Today*, *15*, 171–185.

Murad, A. M., Santiago, F. F., Petroianu, A., Rocha, P. R. S., Rodrigues, M. A. G., & Rausch, M. (1993). Modified therapy with 5-fluorouracil, doxorubicin, and methotrexate in advanced gastric-cancer. *Cancer*, *72*, 37–41.

Natale, R. B., Yagoda, A., Watson, R. C., Whitmore, W. F., Blumenreich, M., & Braun, D. W. (1981). Methotrexate – An active-drug in bladder-cancer. *Cancer*, *47*, 1246–1250.

Richardson, S., Ferruti, P., & Duncan, R. (1999). Poly(amidoamine)s as potential endosomolytic polymers: Evaluation in vitro and body distribution in normal and tumor bearing animals. *Journal of Drug Targeting*, *6*, 391–404.

Roberts, J. C., Bhalgat, M. K., & Zera, R. T. (1996). Preliminary biological evaluation of polyamidoamine (PAMAM) starburst dendrimers. *Journal of Biomedical Materials Research*, *30*, 53–65.

Santos, M. A., Enyedy, E. A., Nuti, E., Rossello, A., Krupenko, N. I., & Krupenko, S. A. (2007). Methotrexate gamma-hydroxamate derivatives as potential dual target antitumor drugs. *Bioorganic & Medicinal Chemistry*, *15*, 1266–1274.

Saovapakhiran, A., D'Emanuele, A., Attwood, D., & Penny, J. (2009). Surface modification of PAMAM dendrimers modulates the mechanism of cellular internalization. *Bioconjugate Chemistry*, *20*, 693–701.

Semberova, J., De Paoli Lacerda, S. H., Simakova, O., Holada, K., Gelderman, M. P., & Simak, J. (2009). Carbon nanotubes activate blood platelets by inducing extracellular Ca^{2+} influx sensitive to calcium entry inhibitors. *Nano Letter*, *9*, 3312–3317.

Simak, J., Gelderman, M. P., Yu, H., Wright, V., & Baird, A. E. (2006). Circulating endothelial microparticles in acute ischemic stroke: A link to severity, lesion volume and outcome. *Journal of Thrombosis and Haemostasis*, *4*, 1296–1302.

Soto-Castro, D., Cruz-Morales, J. A., Apan, M. T. R., & Guadarrama, P. (2012). Solubilization and anticancer-activity enhancement of methotrexate by novel dendrimeric nanodevices synthesized in one-step reaction. *Bioorganic Chemistry*, *41–42*, 13–21.

Svenson, S. (2009). Dendrimers as versatile platform in drug delivery applications. *European Journal of Pharmaceutics and Biopharmaceutics*, *71*, 445–462.

Wan, K. W., Malgesini, B., Verpilio, I., Ferruti, P., Griffiths, P. C., Paul, A., et al. (2004). Poly(amidoamine) salt form: Effect on pH dependent membrane activity and polymer conformation in solution. *Biomacromolecules*, *5*, 1102–1109.

Wang, B. B., Luo, Y. F., Jia, X. R., Gong, Y. M., Ji, Y., Yang, L., et al. (2004). Synthesis and characterization of fan-shape PAMAM dendrons. *Acta Polymerica Sinica*, *2*, 304–308.

Yu, H., Nie, Y., Dohmen, C., Li, Y., & Wagner, E. (2011). Epidermal growth factor-PEG functionalized PAMAM–pentaethylenehexamine dendron for targeted gene delivery produced by click chemistry. *Biomacromolecules*, *12*, 2039–2047.

Ziemba, B., Halets, I., Shcharbin, D., Appelhans, D., Voit, B., Pieszynski, I., et al. (2012). Influence of fourth generation poly(propyleneimine) dendrimers on blood cells. *Journal of Biomedical Materials Research Part A*, *100A*, 2870–2880.